

# Polarized $J/\psi$ Production at CLEO

Seungwon Baek<sup>\*(a)</sup>, P. Ko<sup>†(b)</sup>, Jungil Lee<sup>‡(a)</sup>, and H.S. Song<sup>§(a)</sup>

<sup>(a)</sup> *Center for Theoretical Physics and Department of Physics,  
Seoul National University, Seoul 151-742, Korea*

<sup>(b)</sup> *Department of Physics, KAIST, Taejon 305-701, Korea*

## Abstract

Polarizations of the prompt  $J/\psi$ 's produced in the  $e^+e^-$  annihilation at CLEO energy ( $\sqrt{s} = 10.58$  GeV) are considered in the framework of NRQCD factorization formalism. We find that the  $J/\psi$  polarization has strong dependence on the production mechanism. At CLEO energy, the most dominant  $J/\psi$  production mechanism in the most phase space is the color-singlet mechanism,  $e^+e^- \rightarrow J/\psi + gg$ , for which  $J/\psi$ 's are highly longitudinally polarized. On the other hand, the dominant  $J/\psi$  production mechanism at the upper end point of  $J/\psi$  energy distribution is the color-octet process,  $e^+e^- \rightarrow (c\bar{c})^{(8)} + g$ , for which  $J/\psi$ 's are almost unpolarized. Thus, the measurement of the polarization of the end point  $J/\psi$ 's can give another test of color-octet mechanism, and constraint on the NRQCD matrix elements.

---

\*Electronic address: swbaek@phya.snu.ac.kr

†Electronic address: pko@chep6.kaist.ac.kr

‡Address after Dec. 1, 1997: Dep. of Physics, Ohio State Univ., Columbus, OH 43210, USA.

§Electronic address: hssong@physs.snu.ac.kr

The nonrelativistic QCD(NRQCD) [1] is an effective field theory of QCD that describes heavy quarkonium physics. It has a distinctive feature that allows color-octet mechanism in heavy quarkonium production and decay. After Braaten and Fleming suggested the color-octet mechanism as a possible solution to the  $\psi'$  anomaly at the Tevatron [2], this idea has given possible explanations on several experimental data which could not be explained on the basis of color-singlet model (CSM) [3] [4]. One crucial feature of the NRQCD approach is that a set of universal nonperturbative NRQCD matrix elements describes vastly different heavy quarkonium production and decay processes. These nonperturbative parameters can be extracted from some experimental data or from lattice simulations [5], and then they can be used at other procedures. Thus, one can check consistency of the whole approach based on the NRQCD factorization formalism. In view of this, it is important to calculate as many independent heavy quarkonium production and decay processes as possible, and see if one can have a consistent picture of overall phenomenology for heavy quarkonium physics.

One such process is the inclusive  $J/\psi$  production in the  $e^+e^-$  annihilation,  $e^+e^- \rightarrow J/\psi + X$ , which has been studied in various frameworks. Fritzsche and Kühn [6] studied the process  $e^+e^- \rightarrow J/\psi + g$  as the leading order contribution to the inclusive  $J/\psi$  production subprocess in the color evaporation model. This process was considered in the CSM by various authors [7]. Braaten and Chen [8] showed that the color-octet contribution may dominate near the upper end point of the  $J/\psi$  energy spectrum. In this region, the  $J/\psi$  angular distribution can change dramatically due to the color-octet mechanism. Cho and Leibovich studied this process via color-singlet mechanism in the NRQCD including complete  $\alpha_s^2$  correction [9]. And Yuan, Qiao and Chao studied this process via both color-singlet and color-octet mechanisms, and tried to extract the color-octet matrix elements [10]. Finally, other related processes such as  $e^+e^- \rightarrow J/\psi + \gamma$  and  $e^+e^- \rightarrow J/\psi + e^+e^-$  were considered by Chang *et al.* [11].

In this paper, we consider the  $J/\psi$  polarization in the  $e^+e^-$  annihilation at the CLEO energy ( $\sqrt{s} = 10.58$  GeV). The longitudinal polarization of the prompt  $J/\psi$  is expected to be 42% when the color-octet  $c\bar{c}[^1S_0$  or  $^3P_J]^{(8)}$  contributions are included, whereas the CSM alone predicts 53%. We show that the energy dependence of the longitudinal polarization is sensitive to the  $J/\psi$  production mechanism. If the color-octet mechanism dominates at the upper end point of phase space, almost unpolarized  $J/\psi$ 's are produced. If the color-singlet mechanism dominates, almost longitudinally polarized  $J/\psi$ 's are produced.

In order to study the polarization of  $J/\psi$ 's produced in the  $e^+e^-$  annihilation, we define an observable  $\eta(z)$  as

$$\eta(z) \equiv \frac{d\sigma_L}{dz} / \frac{d\sigma}{dz}, \quad (1)$$

where  $z \equiv 2E_{J/\psi}/\sqrt{s}$ ,  $d\sigma_L/dz$  represents the energy spectrum of the longitudinally polarized prompt  $J/\psi$ , and  $d\sigma/dz$  that of total  $J/\psi$  production. Polarization of produced  $J/\psi$ 's can be obtained by measuring the angular distribution of lepton pair in the subsequent decay of the produced  $J/\psi$ . That is, the angular distribution of decaying leptons in the process,  $J/\psi \rightarrow l^+l^-$ , is given by

$$\frac{d\Gamma}{d\cos\theta_l^*} \propto [1 + \alpha(z) \cos^2\theta_l^*], \quad (2)$$

with  $\theta_l^*$  the angle between the lepton three-momentum in the  $J/\psi$  rest frame and the  $J/\psi$  direction in the lab frame. The relation between  $\alpha$  and  $\eta$  is given by the following equation

$$\alpha(z) = \frac{1 - 3\eta(z)}{1 + \eta(z)}. \quad (3)$$

Therefore, the unpolarized  $J/\psi$  corresponds to  $\eta = 1/3$  ( $\alpha = 0$ ), whereas the pure transverse polarization corresponds to  $\eta = 0$  ( $\alpha = 1$ ).

The dominant color-singlet contributions come from the following two processes:

$$e^+e^- \rightarrow (c\bar{c})[{}^3S_1]^{(1)} + gg \quad (4)$$

$$e^+e^- \rightarrow (c\bar{c})[{}^3S_1]^{(1)} + c\bar{c}. \quad (5)$$

Among color-octet contributions, the following two processes are dominant.

$$e^+e^- \rightarrow (c\bar{c})[{}^1S_0 \text{ or } {}^3P_J]^{(8)} + g \quad (6)$$

$$e^+e^- \rightarrow (c\bar{c})[{}^3S_1]^{(8)} + q\bar{q}. \quad (7)$$

We show the angular momentum and spin quantum numbers of the  $c\bar{c}$  in the spectroscopy notation, and the superscripts (1) and (8) represent its color structures. These  $c\bar{c}[{}^{2S+1}L_J]^{1,8}$  states will eventually evolve into a physical  $J/\psi$  by emitting/absorbing soft gluons, the probabilities for which are parametrized in terms of NRQCD matrix elements,  $\langle O_{1,8}^{J/\psi}({}^{2S+1}L_J) \rangle$ .

We have calculated the cross section for the longitudinal  $J/\psi$  as well as the total cross section for  $J/\psi$  production in the  $e^+e^-$  annihilations, and the full expressions are given in the Appendix. The virtual  $Z^0$  contributions were neglected, which should be a good approximation if  $\sqrt{s}$  is far below  $M_Z$ <sup>1</sup>. Our results for the total production cross sections agree with the previous results obtained in Refs. [9] and [10]<sup>2</sup>.

For numerical analyses, we use the following numbers for nonperturbative matrix elements that appear in the NRQCD factorization formula for the  $J/\psi$  production cross sections :

$$\langle \mathcal{O}_1^{J/\psi}({}^3S_1) \rangle = 0.73 \text{ GeV}^3 \quad (8)$$

$$\langle \mathcal{O}_8^{J/\psi}({}^3S_1) \rangle = 0.015 \text{ GeV}^3 \quad (9)$$

$$\langle \mathcal{O}_8^{J/\psi}({}^1S_0) \rangle \approx 10^{-2} \text{ GeV}^3 \quad (10)$$

$$\langle \mathcal{O}_8^{J/\psi}({}^3P_0) \rangle / m_c^2 \approx 10^{-2} \text{ GeV}^3. \quad (11)$$

We set  $\alpha_s(2m_c) = 0.28$  with  $m_c = 1.48 \text{ GeV}$ .

In Fig 1, we show the  $J/\psi$  production cross sections for different  $J/\psi$  production mechanisms as functions of the beam energy,  $E_{\text{beam}}$ . At low electron-beam energies ( $E_{\text{beam}} < 10 \text{ GeV}$ ) such as CLEO, the color-octet process (6) and the color-singlet process (4) dominate

<sup>1</sup>See Refs. [4] [12] for  $Z^0 \rightarrow J/\psi + X$  at LEP, Ref. [13] for the  $J/\psi$  polarization therein.

<sup>2</sup>There are some typos in the overall factors of Eqs.(3.8),(A2a) and (A2b) in Ref. [9]. Their results should be multiplied by a factor of 3.

over other mechanisms. As the beam energy increases, the cross section via (4) decreases very rapidly, proportional to inverse fourth of the beam energy ( $\propto E_{\text{beam}}^{-4}$ ). And if the beam energy is greater than about 10 GeV, the quark process, which decreases according to the inverse square of the beam energy ( $\propto E_{\text{beam}}^{-2}$ ), dominates as shown in Fig 1. The hard gluon process Eq. (6) dominates when the electron-beam energy is lower than about 10 GeV, and the gluon fragmentation process Eq. (7) dominates when the electron-beam energy is higher than 10 GeV [10].

In Fig. 2, we show the energy distribution ( $d\sigma/dz$ ) of the prompt  $J/\psi$  produced at CLEO, where  $E_{\text{beam}} = 5.29$  GeV and  $z$  is the energy fraction  $E_{J/\psi}/E_{\text{beam}}$  in  $e^+e^-$  center of mass frame. As shown in Fig. 2, the  $J/\psi$ 's produced via the color-singlet gluon mode (4) are roughly three times more than those via the color-singlet charm-quark fragmentation (5). The color-octet contribution is suppressed relative to the color-singlet processes except at the upper end point of phase space, where the color-octet process (6) dominates [8].

In Fig. 3, we show the polarizations of  $J/\psi$ 's for each production mechanism. It turns out that each production mechanism leads to vastly different polarization of  $J/\psi$ 's. The color-singlet gluon mode (4) makes longitudinally polarized  $J/\psi$ 's, so that  $\alpha(z)$  is negative in all the range of  $z$ . Especially, the high energy  $J/\psi$ 's made by (4) are almost completely longitudinally polarized ( $\alpha \rightarrow -1$ ). The  $J/\psi$ 's produced via the color-octet mechanism (6) are populated only at the point region of phase space, since it is a two-body process at the parton level. And they are almost unpolarized ( $\eta = 0.35$ , or equivalently,  $\alpha = -0.05$ ). The  $J/\psi$ 's via the color-octet gluon fragmentation process (7) tend to be transversely polarized over all their energy range, and they become completely transversely polarized at the end-point region. However since this process is not dominant at CLEO energy, we do not consider it anymore. In Fig. 3, we can see that at the upper end point of phase space, if the color-octet process (6) dominates,  $\alpha \approx -0.05$ , and if the color-singlet process (4) dominates,  $\alpha \approx -0.86$ . The  $J/\psi$  polarization at the end point region at CLEO depends on the matrix elements of NRQCD as follows:

$$\alpha = \frac{-0.05\langle\mathcal{O}_8^{J/\psi}(^1S_0)\rangle - 0.82\langle\mathcal{O}_1^{J/\psi}(^3S_1)\rangle - 4.8\langle\mathcal{O}_8^{J/\psi}(^3P_0)\rangle/m_c^2}{19.0\langle\mathcal{O}_8^{J/\psi}(^1S_0)\rangle + 0.94\langle\mathcal{O}_1^{J/\psi}(^3S_1)\rangle + 72.0\langle\mathcal{O}_8^{J/\psi}(^3P_0)\rangle/m_c^2}. \quad (12)$$

So the precise measurement of the  $J/\psi$  polarizations near the end point region at CLEO may provide us with another information on NRQCD matrix elements. In particular, any appreciable deviation from  $\alpha(\text{singlet}) = -0.86$  may be a signal of importance of color-octet mechanism. Finally in Fig. 4, we show  $\alpha(z)$  obtained by summing all the contributions from various  $J/\psi$  production mechanisms at CLEO energy.

Finally, let us remark on the possible breakdown of NRQCD near the end point region of phase space that was recently pointed out by Beneke, Rothstein and Wise [14]. The channel that might have this problem is the  $e^+e^- \rightarrow (c\bar{c})[^1S_0 \text{ or } ^3P_J]^{(8)} + g$  mode. If we consider the soft gluon emission during the evolution of the color-octet  $(c\bar{c})^{(8)}$  states into  $J/\psi$ , the  $z$ -distribution given in Ref. [8] would be changed schematically to the following form :

$$\frac{d\sigma}{dz}(e^+e^- \rightarrow (c\bar{c})[^1S_0]^{(8)} + g) = \int dy_E \frac{d\Omega}{4\pi} \delta(z - (1 + \delta^2/4) - y_E) C_s \frac{3}{4} (1 + \cos^2 \theta) F[^1S_0^{(8)}](y_E), \quad (13)$$

where  $C_s$  is defined in the Appendix (see Eq. (22)), and the shape function  $F$  is given by [14]

$$F[{}^1S_0^{(8)}](y_E) = \sum_X \langle 0 | \psi^\dagger T^a \chi | H + X \rangle \langle H + X | \delta(y_E - (1 - \frac{\delta^2}{4}) in \cdot \hat{D}) \chi^\dagger T^a \psi | 0 \rangle. \quad (14)$$

This shape function  $F[{}^1S_0^{(8)}]$  represents the distribution of energy fraction carried away by soft gluons during the hadronization of the color-octet  $c\bar{c}({}^1S_0)^{(8)}$  pair into the physical  $J/\psi$ , in the  $J/\psi$  rest frame [14]. However,  $C_s$  is independent of the variable  $z$ , and

$$\int dy_E F[{}^1S_0^{(8)}](y_E) = \langle 0 | \mathcal{O}_8^H({}^1S_0) | 0 \rangle. \quad (15)$$

Therefore, the average over some small region near the end point gives just the NRQCD form. This is different from the case of hadroproduction discussed in Ref. [14]. The same argument applies to  $c\bar{c}[{}^3P_0]^{(8)}$  modes, and also to the  $J/\psi$  polarization as well.

In conclusion, we showed that the  $J/\psi$  polarization depends distinctively on the  $J/\psi$  production mechanisms. At the upper end point of phase space where  $J/\psi$ 's are dominantly produced via the color-octet mechanism  $e^+e^- \rightarrow (c\bar{c})_8 + g$ , the measurement of the  $J/\psi$  polarization can give another test of the color-octet mechanism and another constraint on the NRQCD matrix elements. We also argued that the possible breakdown of NRQCD near the phase space boundary does not affect our predictions made in this work. The ongoing data analysis at CLEO will shed light on the relevance of the color-octet mechanism in  $J/\psi$  productions through the measurements of the polar angle distribution and polarization of  $J/\psi$ 's in the  $e^+e^-$  annihilation at CLEO [15].

## ACKNOWLEDGMENTS

We are grateful to K.T. Chao, Victor Kim and M.B. Wise for useful discussions. This work is supported in part by KOSEF through CTP, BSRI-97-2418, and Nondirected Research by Ministry of Education (PK), and KOSEF Fellowship (JL).

## I. APPENDIX

We list the analytic expressions for the differential cross sections of total and longitudinal  $J/\psi$  productions in terms of

$$z = 2E_{J/\psi}/\sqrt{s}, \quad \text{and} \quad \delta = 4m_c/\sqrt{s}.$$

### A. $e^+e^- \rightarrow c\bar{c}[{}^3S_1]^{(1)} + gg$

$$\begin{aligned} \frac{d\sigma_{tot}}{dz}(e^+e^- \rightarrow c\bar{c}[{}^3S_1]^{(1)} gg) &= \frac{8\pi (\alpha\alpha_s e_Q)^2}{81 \delta E_{beam}^5} \frac{\langle \mathcal{O}_1^\psi({}^3S_1) \rangle}{(2-z)^2(2z-\delta^2)^3} \\ &\times \left\{ 4 \left[ -16z^3 + 2z^2(7\delta^2 + 26) - 6z(\delta^2 + 2)(\delta^2 + 4) \right. \right. \\ &\quad \left. \left. + \delta^6 + 7\delta^4 + 20\delta^2 + 16 \right] (2z - \delta^2) \sqrt{z^2 - \delta^2} \right\} \end{aligned}$$

$$\begin{aligned}
& + \left[ 2z^2(5\delta^4 - 4\delta^2 - 16) + 2z\delta^2(-3\delta^4 - 4\delta^2 + 40) \right. \\
& \quad \left. - \delta^2(4 - \delta^2)(\delta^4 + 8\delta^2 + 4) \right] (4z - 4 - \delta^2) \ln \frac{2z - \delta^2 + 2\sqrt{z^2 - \delta^2}}{2z - \delta^2 - 2\sqrt{z^2 - \delta^2}} \Big\}. \tag{16}
\end{aligned}$$

$$\begin{aligned}
\frac{d\sigma_L}{dz}(e^+e^- \rightarrow c\bar{c}[^3S_1]^{(1)}gg) &= \frac{\pi}{324} \frac{(\alpha\alpha_s e_Q)^2}{\delta E_{\text{beam}}^5} \frac{\langle \mathcal{O}_1^\psi(^3S_1) \rangle}{(2-z)^2(2z-\delta^2)^3(z^2-\delta^2)} \\
&\times \left\{ 4 \left[ 128z^4 + 64z^3(\delta^4 - 2\delta^2 + 8) - 32z^2(2\delta^6 + 3\delta^4 + 40\delta^2 + 16) \right. \right. \\
&\quad + 8z\delta^2(3\delta^6 + 4\delta^4 + 128\delta^2 + 128) - \delta^4(3\delta^6 + 4\delta^4 + 144\delta^2 + 576) \Big] (2z - \delta^2) \sqrt{z^2 - \delta^2} \\
&\quad - (4z - \delta^2 - 4) \left[ 64z^4(\delta^4 + 4\delta^2 + 16) + 32z^3\delta^2(-3\delta^4 - 12\delta^2 - 80) \right. \\
&\quad + 8z^2\delta^2(9\delta^6 + 8\delta^4 + 256\delta^2 - 64) + 8z\delta^4(-3\delta^6 - 64\delta^2 + 128) \\
&\quad \left. \left. - \delta^6(4 - \delta^2)(3\delta^4 + 8\delta^2 + 144) \right] \ln \frac{2z - \delta^2 + 2\sqrt{z^2 - \delta^2}}{2z - \delta^2 - 2\sqrt{z^2 - \delta^2}} \right\}. \tag{17}
\end{aligned}$$

**B.  $e^+e^- \rightarrow c\bar{c}[^3S_1]^{(1)} + c\bar{c}$**

$$\begin{aligned}
\frac{d\sigma_{\text{tot}}}{dz}(e^+e^- \rightarrow c\bar{c}[^3S_1]^{(1)}c\bar{c}) &= \frac{\pi}{486} \frac{(\alpha\alpha_s e_Q)^2 \langle \mathcal{O}_1^\psi(^3S_1) \rangle}{\delta^3 E_{\text{beam}}^5 z^3(2-z)^6} \\
&\times \left\{ 4z \sqrt{\frac{(1-z)(z^2-\delta^2)}{4+\delta^2-4z}} \left[ 1280z^8 + 32z^7(\delta^2 - 336) \right. \right. \\
&\quad + 8z^6(-15\delta^4 + 20\delta^2 + 4512) \\
&\quad + 4z^5(3\delta^6 + 136\delta^4 - 512\delta^2 - 13312) \\
&\quad + z^4(-3\delta^8 + 12\delta^6 - 672\delta^4 + 1792\delta^2 + 38912) \\
&\quad + 4z^3(\delta^8 - 12\delta^6 - 288\delta^4 - 2432\delta^2 - 4096) \\
&\quad - 16z^2(\delta^2 + 4)(\delta^6 - 42\delta^4 - 328\delta^2 - 64) \\
&\quad + 16z\delta^2(-3\delta^6 - 88\delta^4 - 576\delta^2 - 1024) \\
&\quad \left. \left. + 16\delta^2(\delta^2 + 4)(\delta^2 + 8)(3\delta^2 + 8) \right] \right. \\
&\quad + \left[ -512z^5 + 8z^4(7\delta^2 + 104) + 8z^3\delta^2(-5\delta^2 - 4) \right. \\
&\quad \left. + z^2(3\delta^6 + 32\delta^4 - 32\delta^2 - 256) + 128z\delta^2(-\delta^2 - 4) + 4\delta^2(3\delta^4 + 32\delta^2 + 64) \right. \\
&\quad \left. \left. \right] \delta^2(2-z)^4 \ln \frac{z\sqrt{4+\delta^2-4z} + 2\sqrt{(1-z)(z^2-\delta^2)}}{z\sqrt{4+\delta^2-4z} - 2\sqrt{(1-z)(z^2-\delta^2)}} \right\}. \tag{18}
\end{aligned}$$

$$\begin{aligned}
\frac{d\sigma_L}{dz}(e^+e^- \rightarrow c\bar{c}[^3S_1]^{(1)}c\bar{c}) &= \frac{\pi}{1458} \frac{(\alpha\alpha_s e_Q)^2 \langle \mathcal{O}_1^\psi(^3S_1) \rangle}{\delta^3 E_{\text{beam}}^5 z^3(2-z)^6(z^2-\delta^2)} \\
&\times \left\{ 4z \sqrt{\frac{(1-z)(z^2-\delta^2)}{4+\delta^2-4z}} \left[ 768z^{10} + 96z^9(\delta^2 - 80) \right. \right.
\end{aligned}$$

$$\begin{aligned}
& +8z^8(9\delta^4 - 116\delta^2 + 3680) \\
& +4z^7(-39\delta^6 - 204\delta^4 + 1696\delta^2 - 11776) \\
& +2z^6(15\delta^8 + 732\delta^6 + 1088\delta^4 - 15104\delta^2 + 18432) \\
& +16z^5(-17\delta^8 - 304\delta^6 - 112\delta^4 + 2240\delta^2 - 1024) \\
& +z^4(3\delta^{10} + 800\delta^8 + 8272\delta^6 + 9600\delta^4 + 512\delta^2 + 4096) \\
& +4z^3\delta^2(-\delta^8 - 296\delta^6 - 1440\delta^4 - 1984\delta^2 - 5120) \\
& +16z^2\delta^2(\delta^8 - 4\delta^6 - 456\delta^4 - 800\delta^2 + 512) \\
& +48z\delta^4(\delta^6 + 40\delta^4 + 272\delta^2 + 384) \\
& +48\delta^4(-\delta^6 - 24\delta^4 - 112\delta^2 - 128) \Big] \\
& -3\delta^2(2-z)^4 \ln \frac{z\sqrt{4+\delta^2-4z} + 2\sqrt{(1-z)(z^2-\delta^2)}}{z\sqrt{4+\delta^2-4z} - 2\sqrt{(1-z)(z^2-\delta^2)}} \Big[ \\
& 8z^6(\delta^2 - 40) + 28z^5\delta^2(-\delta^2 + 8) + 2z^4(5\delta^6 + 24\delta^4 + 144\delta^2 + 128) \\
& +4z^3\delta^4(-7\delta^2 - 36) + z^2\delta^2(\delta^6 + 12\delta^4 - 96\delta^2 - 256) \\
& +16z\delta^4(-3\delta^2 - 8) + 4\delta^4(\delta^4 + 20\delta^2 + 32) \Big] \Big\}. \tag{19}
\end{aligned}$$

**C.**  $e^+e^- \rightarrow c\bar{c}[{}^3S_1]^{(8)} + q\bar{q}$

$$\begin{aligned}
\frac{d\sigma_{tot}}{dz}(e^+e^- \rightarrow c\bar{c}[{}^3S_1]^{(8)}q\bar{q}) &= \frac{\pi}{72} \frac{\langle \mathcal{O}_8^\psi({}^3S_1) \rangle}{m_c^3 E_{beam}^2} (\alpha\alpha_s e_Q)^2 \\
&\times \left[ \log \left( \frac{z + \sqrt{z^2 - \delta^2}}{z - \sqrt{z^2 - \delta^2}} \right) \left\{ 4z - 2(4 + \delta^2) + \frac{(4 + \delta^2)^2}{2z} \right\} - 8\sqrt{z^2 - \delta^2} \right]. \tag{20}
\end{aligned}$$

$$\begin{aligned}
\frac{d\sigma_L}{dz}(e^+e^- \rightarrow c\bar{c}[{}^3S_1]^{(8)}q\bar{q}) &= \frac{\pi}{72} \frac{\langle \mathcal{O}_8^\psi({}^3S_1) \rangle}{m_c^3 E_{beam}^2} (\alpha\alpha_s e_Q)^2 \\
&\times \frac{(4z - (4 + \delta^2))(4 + \delta^2)}{2(z^2 - \delta^2)} \left[ \log \left( \frac{z + \sqrt{z^2 - \delta^2}}{z - \sqrt{z^2 - \delta^2}} \right) / 2z - \sqrt{z^2 - \delta^2} \right]. \tag{21}
\end{aligned}$$

**D.**  $e^+e^- \rightarrow c\bar{c}[{}^1S_0 \text{ or } {}^3P_0]^{(8)} + g$

$$\sigma(e^+e^- \rightarrow c\bar{c}[{}^1S_0 \text{ or } {}^3P_0]^{(8)}g) = C_S \langle \mathcal{O}_8^\psi({}^1S_0) \rangle + C_P \langle \mathcal{O}_8^\psi({}^3P_0) \rangle, \text{ where} \tag{22}$$

$$\begin{aligned}
C_S &= \frac{8\pi^2\alpha^2 e_Q^2 \alpha_s}{3s^2 m_c} (4 - \delta^2), \\
C_S^{long} &= C_S/3, \\
C_P &= \frac{8\pi^2\alpha^2 e_Q^2 \alpha_s}{3s^2 m_c^3} \frac{48 + 8\delta^2 + 7\delta^4}{4 - \delta^2}, \\
C_P^{long} &= \frac{8\pi^2\alpha^2 e_Q^2 \alpha_s}{3s^2 m_c^3} \frac{(4 + \delta^2)^2}{4 - \delta^2}. \tag{23}
\end{aligned}$$

Here,  $C_{S,P}^{long}$  correspond to the longitudinal  $J/\psi$  production.

## REFERENCES

- [1] G. T. Bodwin, E. Braaten and G. P. Lepage, Phys. Rev. D**51**, 1125 (1995).
- [2] E. Braaten and S. Fleming, Phys. Rev. Lett. **74**, 3327 (1995).
- [3] P. Ko, Jungil Lee and H.S. Song, Phys. Rev. D **53**, 1409 (1996).
- [4] K. Cheung, W.-Y. Keung and T. C. Yuan, Phys. Rev. Lett. **76**, 877 (1996) ; P. Cho, Phys. Lett. **B 368**, 171 (1996) ; S. Baek, P. Ko, Jungil Lee and H.S. Song, Phys. Lett. **B 389**, 609 (1996).
- [5] G. T. Bodwin, D. K. Sinclair, S. Kim, Phys. Rev. Lett. **77**, 2376 (1996).
- [6] H. Fritzsche and J. H. Kühn, Phys. Lett. **90 B**, 164 (1980).
- [7] J. H. Kühn and H. Schneider, Phys. Rev. D **24**, 2996 (1981) ; J. H. Kühn and H. Schneider, Z. Phys. **C 11**, 253 (1981) ; L. Clavelli, Phys. Rev. D **26**, 1610 (1982) ; V.M. Driesen, J.H. Kühn and E. Mirkes, Phys. Rev. D **49**, 3197 (1994).
- [8] E. Braaten and Y.-Q. Chen, Phys. Rev. Lett. **76**, 730 (1996).
- [9] P. Cho and A. K. Leibovich, Phys. Rev. D **54**, 6690 (1996).
- [10] F. Yuan , C.-F. Qiao and K.-T. Chao, Phys. Rev. D **56**, 321 (1997).
- [11] Chao-Hsi Chang, Cong-Fong Qiao and Jian-Xiong Wang, Phys. Rev. D **56**, 1363 (1997) ; AS-ITP-97-15, hep-ph/9706443 (1997).
- [12] E. Braaten, K. Cheung and T. C. Yuan, Phys. Rev. D **48**, 4230 (1993).
- [13] S. Baek, P. Ko, Jungil Lee and H.S. Song, Phys. Rev. D **55**, 6839 (1997).
- [14] M. Beneke, I. Z. Rothstein and M. B. Wise, Phys. Lett. **B408**, 373 (1997).
- [15] A.H. Wolf, private communications.

## FIGURE CAPTIONS

Fig. 1 The cross section for each mode versus electron beam energy:  $e^+e^- \rightarrow J/\psi + q\bar{q}$  (solid),  $e^+e^- \rightarrow J/\psi + c\bar{c}$  (long-dashed),  $e^+e^- \rightarrow J/\psi + gg$  (short-dashed), and  $e^+e^- \rightarrow J/\psi + g$  (dotted).

Fig. 2 Energy spectra of  $J/\psi$ 's at CLEO energy for each mode :  $e^+e^- \rightarrow J/\psi + gg$ ,  $e^+e^- \rightarrow J/\psi + c\bar{c}$ ,  $e^+e^- \rightarrow J/\psi + q\bar{q}$ , and  $e^+e^- \rightarrow J/\psi + g$ .

Fig. 3  $\alpha(z)$  for each mechanism at CLEO energy.

Fig. 4  $\alpha(z)$  for the sum of all modes at CLEO energy.

FIGURES

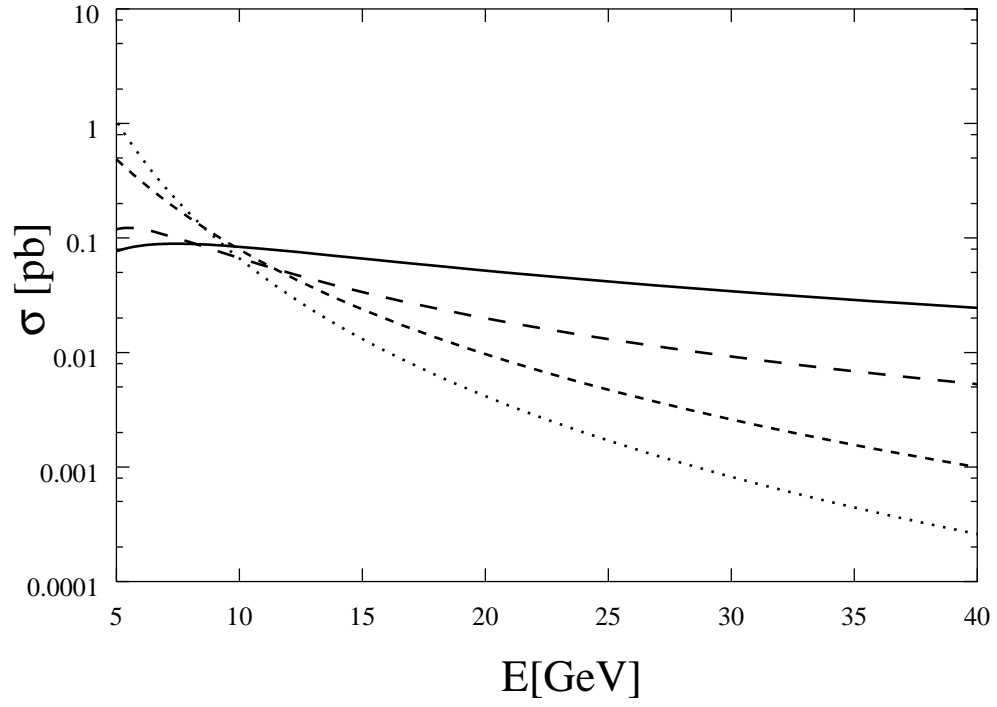


FIG. 1.

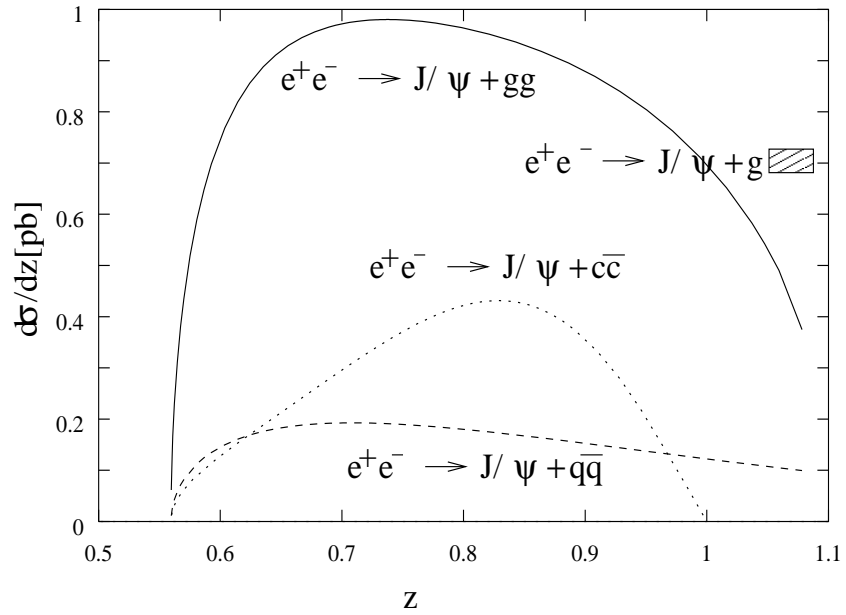


FIG. 2.

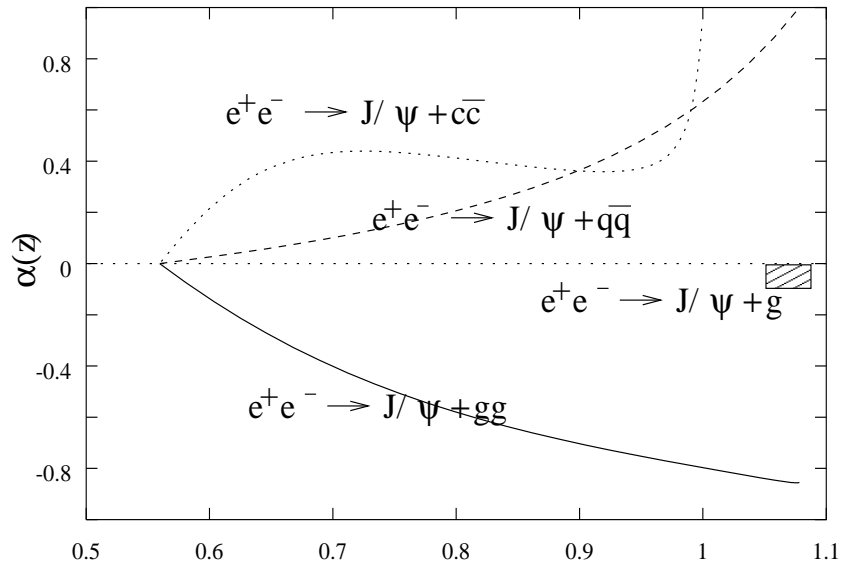


FIG. 3.

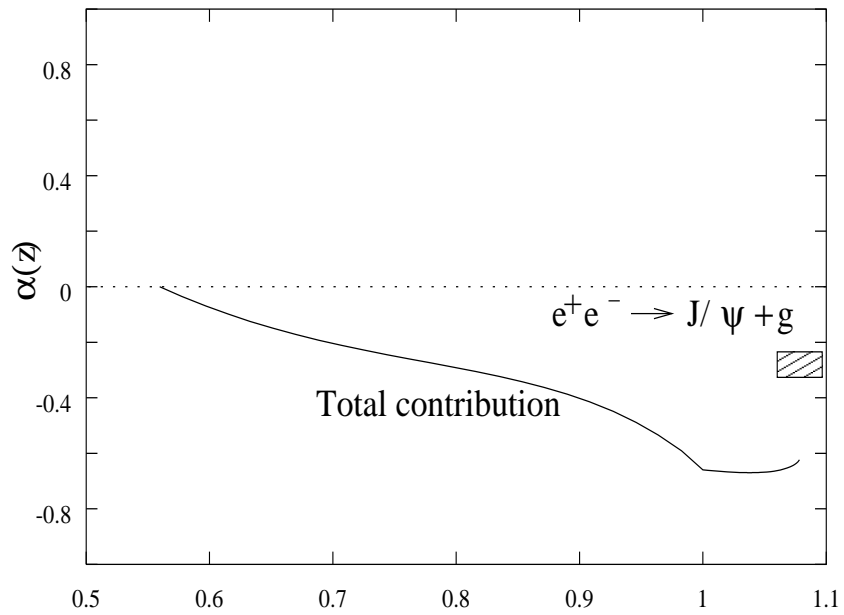


FIG. 4.